*Transactions of the Materials Research Society of Japan* 26 [2] 775-778 (2001)

# *In situ* observation of critical phenomena at surfaces of $Cu_3Au(001)$ and Si(001) near the transition temperatures

MASAO KIMURA
Adv. Tech. Res. Labs., Nippon Steel Corporation,
20-1 Shintomi, Futtsu, Chiba 293-8511, Japan
FAX 81-439-80-2746, e-mail: kimura@re.nsc.co.jp

Surface-induced ordering and disordering near the bulk critical temperature have been investigated by *in situ* observation using evanescent wave. Two opposite-type of phenomena were studied. **Surface-induced ordering** above the bulk critical temperature $T_{c;b}$ was found for the $Cu_3Au$ (001) surface by measuring surface diffuse scattering. Long-range order (LRO) was lost just below $T_{c;b}$, but the short-range order (SRO) remained, showing ordered domains with $\{1\bar{0}\}$ Anti Phase Domain Boundary. **Surface-induced disordering** below the bulk melting temperature $T_{m;b}$ was found for the Si(001) surface by x-ray reflectivity measurements under He-gas. It has been shown that the density of the surface is, in a region of $T_{m;b}$ - 110 K < $T$ < $T_{m;b}$ is larger than that of the bulk solid, which indicates surface melting. Surface-induced ordering and disordering, revealed by *in situ* observation using evanescent wave, give fundamental information to understand surfaces/interfaces.

Key words: *in situ*, order-disorder phase transition, surface-melting, Si, $Cu_3Au$, evanescent wave

## 1. INTRODUCTION

When a surface is irradiated by an x-ray beam with a small angle near its critical angle ($\alpha_c$), the x-ray intensities decrease exponentially along the depth ( "Evanescent Wave", Fig.1). X-ray evanescent wave can reveal change of surface structures by *in situ* observation, which is crucial to understand "real surface/interfaces". Two opposite-type of phenomena: surface-induced ordering and disordering near the bulk critical ($T_{c;b}$) and the bulk melting temperature ($T_{m;b}$) have been investigated by *in situ* observation using evanescent wave.

Order-disorder transformation in $Cu_3Au$ (001) surface has been investigated. The alloy $Cu_3Au$, which orders from the $A1$ to the $L1_2$ structure at the critical temperature $T_{m;b}$ = 663 K, is considered a classic example of an order-disorder phase transformation. The atomic ordering of bulk $Cu_3Au$ above $T_{m;b}$ has been investigated extensively[1,2]. However, only several studies have been made on surfaces[3]. Both surface-induced *ordering* and *disordering* have been reported, and more information is necessary for further investigation.

Another important issue at surfaces is surface melting. Surface melting can be generally recognized as a state that a liquid film is formed and wets the solid-vapor interface at $T_{m;b}$. The surface melting phenomenon of Si has attracted special attention in the last few years. But most work on Si surfaces has focused on their behavior at low and intermediate temperatures[4], and little information is known near $T_{m;b}$. because of the experimental difficulties.

In this study, order-disorder transformation of $Cu_3Au$ (001) surface and surface melting of Si(001) have been investigated by *in situ* observation using evanescent wave. New systems for *in situ* observation have been developed and are described in Sec.2. The results of $Cu_3Au$ (001) and Si(001) are shown in Sec.3 and Sec.4, respectively.

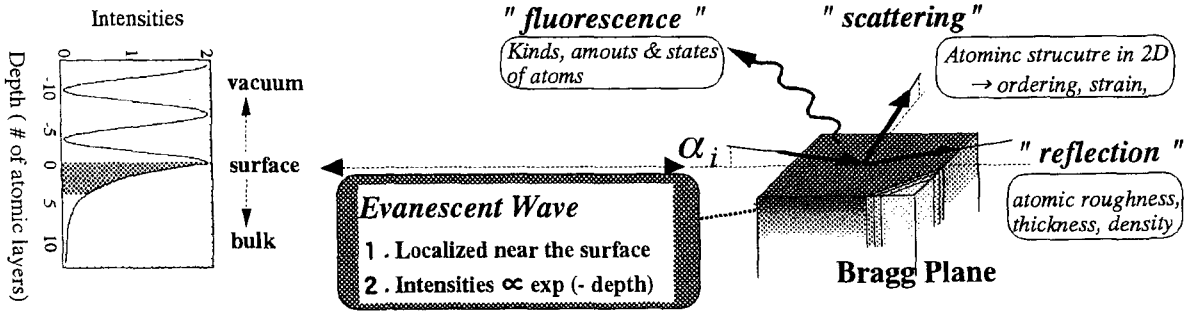


Fig.1 Phenomena caused by evanescent wave

## 2. EXPERIMENTS

A new system is designed for observation of critical phenomena at high temperatures. The system is composed of an *in situ* chamber and x-ray optics for generating evanescent wave and measuring the scattering and reflection from it (Fig.1). A specimen and

heating system were located inside the *in situ* chamber where the atmosphere can be controlled. An x-ray beam from synchrotron radiation was used to measure diffuse intensities and reflectivity of the surface.

2.1 Diffuse intensity measurements of $Cu_3Au$ (001)

The specimen was mounted in a UHV surface x-ray diffraction chamber equipped with LEED, Auger-spectroscopy, and an ion gun for cleaning the specimen by sputtering. The X-ray optics for the experiments include a Ge-(111) monochromator and a Pt-coated focusing mirror. The diffuse intensities were measured at $\alpha_i = 1.2\ \alpha_c$, and $E = 11.819$ keV with a resolution less than 0.02 in the reciprocal lattice. The experiment was performed using beam line X2A at the National Synchrotron Light Source, Brookhaven National Laboratory.

A specimen with a stoichiometric composition (12 mm in diameter and 4 mm in thickness) was prepared, and a mirror-like surface was prepared by mechanically polishing with $Al_2O_3$ to within 0.36° of the (001). Then the specimen was kept at 743 K for a few hours and slowly cooled down to a temperature just below $T_{c;b}$ over several days. Auger-spectroscopy and LEED measurements were examined to assure a clean and well-ordered (001) surface.

2.2 Reflectivity measurements of Si (001)

A part of the *in situ* chamber is shown in Fig.2. A carbon heater ("H" in Fig.2) coated with SiC film was located above the surface of the specimen. The heater, the specimen and the plate were surrounded by an insulator of porous carbon with thickness of about 30 mm ("I" in Fig.2), which made it possible to control the surface temperature as high as $T_{m;b}$ with enough accuracy. The surface temperature can be controlled at a set temperature with an error of less than ± 2-5 degrees up to near $T_{m;b}$, by monitoring two thermocouples (TC1&TC2). A temperature gradient in the near surface region of $10^3$ nm is expected to be smaller than a few degrees.

The reflectivity was measured by an NaI scintillation counter (SC) with $E$ = 6812 eV. Experiments were carried out at a beam line BL-3A at Photon Factory, KEK, in Tsukuba, Japan. In this beam line, an x-ray beam from a bending magnet is monochromated by Si(111) double crystal.

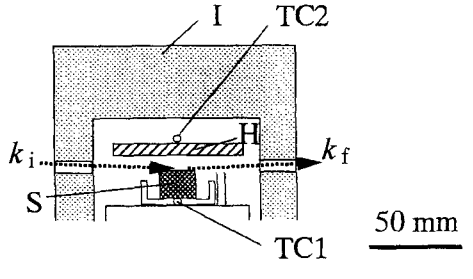


Fig.2 Part of the *in situ* chamber for reflectivity measurements.

## 3. RESULTS OF Cu3Au (001)[5,6]

Measured diffuse intensity (Fig.3) contains short-range order terms and displacement terms, and can be seperated into the terms based on a series expansion of the scattering equation in which terms up to the second order in displacement are retained[7].

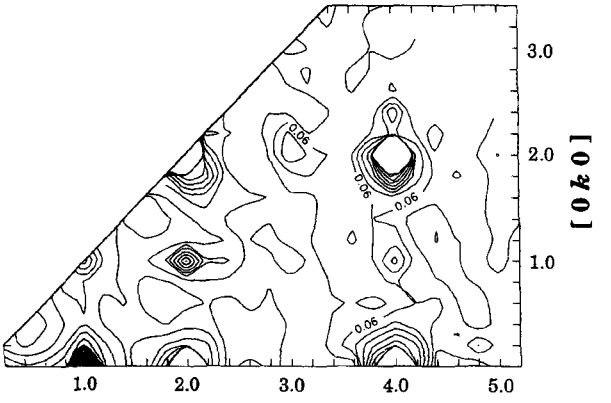


Fig. 3 Contour map of the diffuse intensities in the two-dimensional reciprocal lattice *hk*.

Both terms contain 14 unknown coefficients which are Fourier sum over the inter atomic vectors ($l$, $m$) and correspond to the crystallographic parameters such as SRO and the atomic displacements. Example of the coefficients are :

$$I_{\mathrm{SRO}} = \sum_l \sum_m \alpha_{lm} \cos(2\pi hl) \cos(2\pi km), \tag{1}$$

$$Q_x^{\mathrm{Cu-Cu}} = -2\pi \sum_l \sum_m \left( \frac{c_{\mathrm{Cu}}}{c_{\mathrm{Au}}} + \alpha_{lm} \right) \langle X_{lm}^{\mathrm{Cu-Cu}} \rangle \times \sin(2\pi hl) \cos(2\pi km), \tag{2}$$

$$R_x^{\mathrm{Cu-Cu}} = 4\pi^2 \sum_l \sum_m \left( \frac{c_{\mathrm{Cu}}}{c_{\mathrm{Au}}} + \alpha_{lm} \right) \langle X_{00}^{\mathrm{Cu}} X_{lm}^{\mathrm{Cu}} \rangle \times \cos(2\pi hl) \cos(2\pi km), \tag{3}$$

$$S_{xy}^{\mathrm{Cu-Cu}} = -8\pi^2 \sum_l \sum_m \left( \frac{c_{\mathrm{Cu}}}{c_{\mathrm{Au}}} + \alpha_{lm} \right) \langle X_{00}^{\mathrm{Cu}} X_{lm}^{\mathrm{Cu}} \rangle \times \sin(2\pi hl) \sin(2\pi km), \tag{4}$$

$$\alpha_{lm} = 1 - \frac{P_{lm}^{\mathrm{Au-Cu}}}{c_{\mathrm{Cu}}}, \tag{5}$$

The $\alpha_{lm}$ are the two-dimensional Cowley-Warren short-range-order, where the parameters $P_{lm}^{Au\text{-}Cu}$ are the conditional probabilities of finding a Cu atom at the end of a vector $(a/2)(l,m)$ given an Au atom at its origin. Also, $X_{lm}^{Cu\text{-}Cu}$ represents the projected displacement, along the $x$-axis, of two Cu atoms separated by a vector $(a/2)(l,m)$, and the carats represent lattice averages.

The total diffuse intensity was measured at a set of symmetry related points (20-30 typically) to points in a minimum area where the magnitude of the Fourier sums are the same. The separation was then performed using a least-squares procedure. Once this separation was done for the points in minimum area, real space quantities (SRO parameters: $\alpha_{lm}$, and atomic

displacements: $X_{lm}^{Cu\text{-}Cu}$ ...) could be obtained by Fourier inversion.

Then a computer simulation of the atomic structure of $Cu_3Au$, based on the measured SRO parameters, was performed in two dimensions. A square lattice, 128 by 128 simple cubic cells with periodic boundary conditions was adjusted so that the first five SRO parameters were matched to the measured values within 5-6 % (the LRO parameters were set to zero). A typical portion of the results, composed of 30 by 30 cells, is shown in Fig. 4, where one of the "ordered" domains and the Au-clusters are indicated by the solid and the broken lines, respectively.

The most outstanding features of atomic configurations are: (i) *ordered domains* (with {10} APB (Anti Phase Boundaries) with a unique shape, and (ii) *clusters* composed of the same kind of atoms. This feature is similar to that of the bulk, where there are large concentrations of low energy APB on {100} planes created by 1/2 <110> (001) displacements *in* the boundary planes, which have the lowest APB energy. Thus it appears that the same type of APB plays an important role in the surface, as well.

However the pair potentials obtained by fitting the SRO shows a large attractive force at the nearest neighboring site. This interaction may cause the surface induced-ordering, resulting in the domain structure of the surface above $T_{c;b}$ .

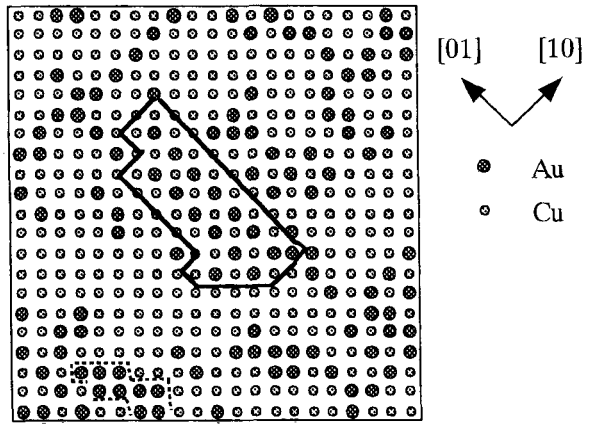


Fig. 4 $Cu_3Au$ (001) surface 56 K above $T_{c;b}$ . Au and Cu atoms are represented by large and small circles, respectively.

## 3. RESULTS OF Si (001)[8]

*In situ* measurements of reflectivity curves were performed at ambient temperature. Some typical changes of reflectivity curves are shown in Fig. 5. The most outstanding change of the curve during heating was a change of the critical angle $a_c$ on heating from $T$ = 1473 to 1573 K, which showed an increase of density of the surface well below $T_{m;b}$,(Fig.5). It should be stressed that this phenomenon was reversible with temperature change; when the temperature was decreased from $T$ = 1623 to 1473 K, the surface density $r$ decreased and returned to the value at 1473 K on heating .

Another change was found in the region where the angle of incidence $a_f > a_c$ ; the degree of decay of reflectivity became larger at $T$ > 1473 K than at $T$ = RT, showing a change of surface roughness from a smooth to a rough surface on heating. This change was not reversible, and the rough surface remained the same even when the temperature was decreased from $T$ = 1623 to 1523 K.

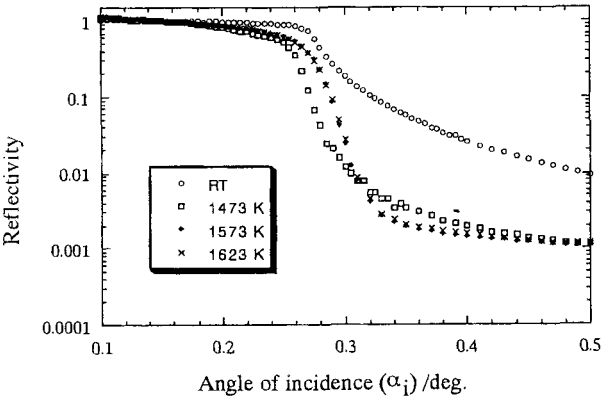


Fig. 5 Change of reflectivity curves obtained by *in situ* observation.

Reflectivity curves obtained at each temperature were analyzed. X-ray reflectivity : $R(Q)$ is the function of the scattering vector $Q$, and is given by[9]

$$R(Q) = R_F(Q)\left|\int \rho'(z)\exp(iQz)dz\right|^2 \quad (6)$$

where $R_F(Q)$ is the Fresnel reflectivity, and ρ'(z) denotes the gradient of normalized density (ρ(z)) along the depth direction.

When the surface is covered by some layers, the reflectivity curve was calculated based on the Vidal and Vincent formalism considering the Gaussian rms microroughness[10].

In the fitting, various models were tried : (1) surface layer of Si / bulk Si, (2) $SiO_2$ / Si, and (3) only bulk Si. The model (1) explains best the reflectivity curves at $T$ > 1570 K, showing the existence of a surface layer with a density of 2.5 (2) × $10^3$ kg/m$^3$ which is larger than that of the bulk substrate ( 2.3 (2) × $10^3$ kg/m$^3$) in a region $T_{m;b}$ - 110 K < $T$ < $T_{m;b}$ . Reflectivity curves obtained at each temperature were analyzed in the same way. The obtained values of density (ρ) of Si(001) surface are plotted as a function of temperature (Fig. 6); error bars show error in determination of ρ, which mainly comes from the measurements of the angle and the fitting procedure .

*In situ* observation showed that the transition temperature of surface melting is located in a range of 1473 K< $T_{m;s}$* < 1573 K = $T_{m;b}$ - 110 K. This temperature is about 20-50 K higher than the temperature range where the atomic disordering was reported to occur. This is consistent with the reported studies that crystallographic anisotropy in the plane becomes almost zero at T=1500 K[11]. Atomic disordering may proceed surface melting. More experiments are required to determine $T_{m;s}$* near the range of 1473 -1573 K.

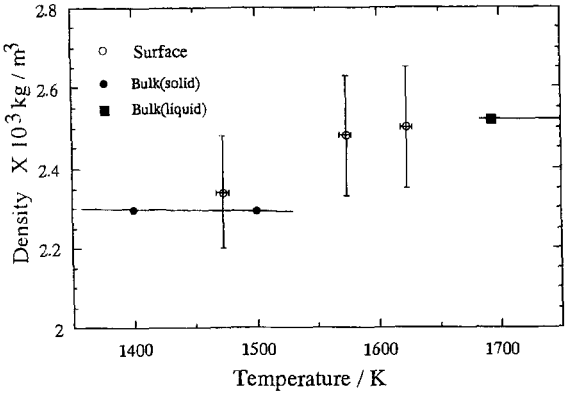


Fig. 6 Temperature dependence of density of Si (001) surface. Open symbols for this study , and closed ones for the bulk. The line is a guide for eye.

Fig. 7 summarizes schematically the phenomena of Si at high temperature, shown by this study and reported ones. Atomic disordering of the surface starts around $T > 1400$ K, and long-range order is almost lost around $T = 1500$ K. Then the atomic state of surface becomes near that of the bulk liquid (surface-melting) at $T > T_{m;s}^*$ (1473 K - 1573 K). The disordering was observed mainly in vacuum, and the surface-melting was observed under He gas, as shown in this study.

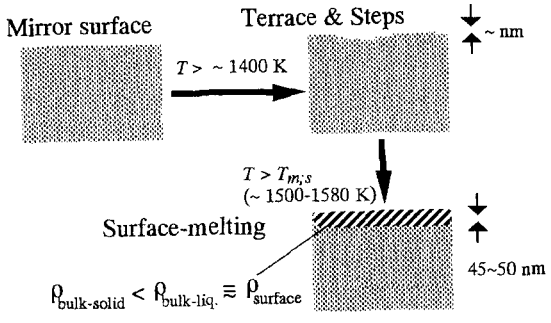


Fig. 7 Schematic diagram of change of Si(001) on heating in He.

Now the possible phenomenon of surface-melting of Si(001) is compared with other systems by comparing the temperature ratio of surface-melting (or metallic-transition) / bulk-melting : $T_{m;s/b}$ is one of the indexes for comparison: $T_{m;s/b}$ . $T_{m;s/b}$ of Si(001) (0.88-0.93) is relatively lower than those of other metals (0.93- 0.98). The uniqueness of surface-melting of Si and Ge can be understood simply in terms of atomic coordination. Si is one fo the semiconductors belonging to IVB in the periodic table, and have a unique binding structure of the diamond-type. The numbers of the nearest neighbors (NN) at $T$ = RT are 4 for Si, where as they are 12 for In, Pb and Al which reportedly show surface melting. In other words, Si is relatively lose-packed, and forms a networking structure of a diamond-type. The Friedle oscillations of the pair potential results in a complex structure of the liquid with low coordination numbers[12].

## 4. CONCLUSION

Surface-induced ordering and disordering near the bulk critical temperature have been investigated by *in situ* observation using evanescent wave. Unique systems for *in situ* observation have been developed and the following phenomena were revealed:

(i) Surface-induced ordering of $Cu_3Au(001)$ surface: LRO was lost just below $T_{c;b}$, but SRO remained and showed ordered domains with {10} APB,

(ii) Surface-induced disordering or surface melting of Si(001) surface: the density of the surface is, in a region of $T_{m;b}$ - 110 K < $T$ < $T_{m;b}$ is larger than that of the bulk solid, which indicates surface melting.

*In situ* observation is essential to understand change in surface structures around phase transitions, because they are sensitive to temperature and atmosphere. It has shown that the advanced approaches with evanescent wave is powerful to reveal them.

The author would like to thank the staff of NSLS and PF for experimental supports. The experiments have been carried out with the colleagues at Northwestern Univ, Exxson Co. Res. Labs. and Nippon Steel Co.

## REFERENCES

1. J. M. Cowley, J. Appl. Phys. **21**, 24 (1950).
2. B. D. Butle and J. B. Cohen, J. Appl. Phys. **65**, 2214 (1989).
3. H. Dosch, *Critical Phenomena at Surfaces and Ineterfaces*Springer Tracts in Modern Physics (Springer-Verlag, Berlin Heideberg, 1992), vol. 126.
4. V. G. Lifshits, A. A. Saranin, A. Z. Zotov, *Surface Phase on Silicon: Preparation, Strucutres, and Properties* (John Wiley & Sons, Chichester, 1994).
5. M. Kimura, J. B. Cohen, S. Chandavarkar, K. Liang, Physica B **221**, 101(1996).
6. M. Kimura, J. B. Cohen, K. Liang, J. Mater. Res. **12**, 75 (1997).
7. L. H. Schwartz, J. B. Cohen, in *Diffraction from Materials, 2nd ed.* (Springer, Berlin, 1978).
8. M. Kimura, A. Ikari, J. Appl. Phys. **89**, 2138 (2001).
9. J. Als-Nielsen, in *Handbook on Synchrotron Radiation* G. Brown, D.-E. Moncton, Eds. (Elsevier Science Publishsers B.V., 1991), vol. 3, pp. Chapt. 12.
10. B. Vidal, P. Vincent, App. Opt. **23**, 1794 (1984).
11. J. J. Metois, D. E. Wolf, Surf. Sci. **298**, 71(1993).
12. W. Jank, J. Hafner, Phys.Rev.B **41**, 1497 (1990).

(Received December 25, 2000; Accepted March 1, 2001)